Research Paper

Real-Time and Non-invasive Monitoring of the Activation of the IRE1α-XBP1 Pathway in Individuals with Hemodynamic Impairment

Baptiste Fohlen [a,b,c,1], Quentin Tavernier [c,e,1], Thi-mum Huynh [a,b,c], Cédric Caradeuc [c,d], Delphine Le Corre [c,e], Gildas Bertho [c,d], Bernard Cholley [a,b,c], Nicolas Pallet [b,c,e,f,g,*]

[a] Department d'Anésthésie et de Réanimation Cardiovasculaire, Hôpital Européen Georges Pompidou, Paris, France
[b] Assistance Publique-Hôpitaux de Paris (APHP), Paris, France
[c] Université Paris Descartes, Paris, France
[d] Centre National pour le Recherche Scientifique (CNRS) U8601, Paris, France
[e] Institut National de la Santé et de la Recherche Médicale (INSERM) U1147, Paris, France
[f] Service de Néphrologie, Hôpital Européen Georges Pompidou, Paris, France
[g] Service de Biochimie, Hôpital Européen Georges Pompidou, Paris, France

ARTICLE INFO

ABSTRACT

Many stressors that are encountered upon kidney injury are likely to trigger endoplasmic reticulum (ER) stress, subsequently activating transcriptional, translational and metabolic reprogramming. Monitoring early cellular adaptive responses engaged after hemodynamic impairment yields may represent a clinically relevant approach. However, a non-invasive method for detecting the ER stress response has not been developed. We combined a metabolomic approach with genetic marker analyses using urine from individuals undergoing scheduled cardiac surgery under cardiopulmonary bypass to investigate the feasibility and significance of monitoring the ER stress response in the kidney. We developed an original method based on fragment analysis that measures urinary levels of the spliced X-box binding protein 1 (sXBP1) mRNA as a proxy of inositol-requiring enzyme 1α (IRE1α) activity because sXBP1 is absolutely sensitive and specific for ER stress. The early engagement of the ER stress response after ischemic stress is critical for protecting against tissue damage, and individuals who mount a robust adaptive response are protected against AKI. The clinical consequences of our findings are of considerable importance because ER stress is involved in numerous conditions that lead to AKI and chronic kidney disease; in addition, the detection of ER stress is straightforward and immediately available in routine practice.

1. Introduction

Medical conditions that ultimately lead to ischemic tissue injury, such as ischemic acute kidney injury (AKI), are accompanied by micro-environmental alterations (nutrients, growth factors and oxygen deprivation) and disturbances in cellular homeostasis (energetic failure) in the kidney, forcing cells to engage adaptive responses to reduce or eliminate the intensity of the stressor, initiate metabolic reprogramming, regulate the fate of the cell by activating both anti- and pro-apoptotic pathways, and activate communication networks with the immune system to signal a problem (Chovatiya and Medzhitov, 2014; Kotas and Medzhitov, 2015). These molecular and cellular adaptive responses occur very early after the initiation of a stressful condition, long before cell death and the initiation of

maladaptive repair processes (Bonventre and Zuk, 2004; Duffield, 2014; Ferenbach and Bonventre, 2015; Zuk and Bonventre, 2016). Therefore, the detection of their activation constitutes an opportunity for the early diagnosis of ongoing tissue injury, which is crucial for the development of preventive and therapeutic strategies in renal medicine.

Endoplasmic reticulum (ER) stress and its adaptive response, the unfolded protein response (UPR), represent an archetypal example of these adaptive stress responses. ER stress and the disruption of ER proteostasis or parts of the UPR that, for instance, affect epithelial cells, actively participate in the development of AKI and chronic kidney disease (CKD) (El Karoui et al., 2016; Inagi et al., 2014; Mami et al., 2016a; Mami et al., 2016b; Zuk and Bonventre, 2016). A wide range of cellular environments and events induce ER stress, including an autophagy deficiency, energy deprivation, limited or excess nutrients, dysregulated calcium levels, perturbations in redox homeostasis, inflammatory challenges and hypoxia, virtually all of which are encountered in medical situations that promote ischemic AKI (Walter and Ron, 2011). Under ER stress conditions, the aim of the UPR is to adapt to the changing environment and reestablish normal ER function by inducing

* Corresponding author at: Service de Biochimie, Hopital Européen Georges Pompidou, 20, rue Leblanc, 75015 Paris, France.
E-mail address: nicolas.pallet@parisdescartes.fr (N. Pallet).
[1] Baptiste Fohlen and Quentin Tavernier are co-first authors.

transcriptional, translational, and metabolic reprogramming (Walter and Ron, 2011; Wang and Kaufman, 2016; Gao et al., 2015; Wellen and Thompson, 2010). Three major mediators are involved in the UPR: ATF6 (activated transcription factor 6), IRE1α (inositol-requiring enzyme 1α) and PERK (protein kinase RNA (PKR)-like ER kinase).

Of particular interest in the UPR is the IRE1α/X-box binding protein-1 (XBP1) axis. The ribonuclease activity of IRE1α catalyzes the unconventional splicing of a 26 nucleotide intron from the mRNA encoding the transcription factor XBP1, creating a transcriptionally active spliced XBP1 (sXBP1). XBP1 protein translated from mammalian unspliced XBP1 mRNA acts as negative regulator by heterodimerizing with the transcription factor sXBP1 to promote its degradation. Genes that are regulated by sXBP1 enhance protein folding, transport, and degradation, expand protein secretory pathways, and rewire cellular energetic metabolism (Wu et al., 2015; Cubillos-Ruiz et al., 2015; Chen et al., 2014; Hetz and Glimcher, 2009). Therefore, the activation of the IRE1α/XBP1 axis protects against ER stress. The clinical (yet unproven) consequence of the activation of this pathway would be that the robust production of sXBP1 induces (and could predict) protection against tissue damage and the detection of sXBP1 may have prognostic value. Since XBP1 splicing depends exclusively on IRE1α activity, sXBP1 is only produced if and when ER stress occurs (with a rare exception), therefore reflecting the presence of ER stress with absolute sensitivity. In some specific cases, IRE1α is not activated by the accumulation of misfolded proteins within the RE: Toll like receptors 2 and 4 activation by microbial products specifically promotes the phosphorylation of IRE1α and the activation of XBP1 (Martinon et al., 2010). In turn, a lack of sXBP1 production virtually eliminates the possibility of activating the IRE1α branch of the UPR.

We performed this proof of concept study to test and validate the hypothesis that the ER stress response to a renal ischemic insult can be non-invasively monitored and provides information about patients' risks of developing AKI. Therefore, we combined a metabolomic approach for monitoring metabolic reprogramming with an original method that measures urinary levels of the sXBP1 mRNA as a readout of IRE1α activity to dynamically and non-invasively monitor renal ER stress. This prospective pilot study was performed in a cohort of individuals undergoing scheduled cardiac surgery under extracorporeal circulation using cardiopulmonary bypass (CPB), a procedure that promotes hemodynamic impairment and ischemic stress in the kidney.

2. Methods

2.1. Patients

From 17 February 2017 to 26 April 2017, 42 patients undergoing scheduled cardiac surgery with CPB were enrolled. The exclusion criteria were: an eGFR < 30 ml/min/1.73 m², infusion of a radio contrast agent within the 24 h before surgery, a preoperative left ventricular ejection fraction <40%, age < 18 years, pregnancy, and the inability to provide consent. AKI was diagnosed according to the KDIGO Clinical Practice Guideline for AKI criteria (http://kdigo.org/) using serum creatinine levels and urine output after the surgery.

2.2. Study Approval

This single-center, prospective, pilot study was approved by the French ethical committee on 7 February 2017 (CPP Sud Est III n° 2016-072 B) and registered under the EudraCT n° 2016-A01871-50. All patients provided written consent for study participation and for the biological analysis before inclusion.

2.3. Surgical Procedure

All medications acting on the renin-angiotensin system and all diuretics were stopped on the day before surgery. General anesthesia was induced according to the protocols of the Anesthesiology Department. Anesthesia was induced and maintained in patients using target-controlled infusions of sufentanil and propofol. Atracurium was used for all anesthetics. Hemodynamic parameters were monitored with a radial artery catheter on a Philips Intellivue® MX 800. Tranexamic acid was injected before and after CPB. The CPB target flow rate was calculated using the following equation: flow (l/min) = 2.6 × body surface area. Heparin was infused before and during CPB to achieve and maintain an activated clotting time > 400 s. The protamine dose was calculated at a 1:1 rate of the heparin dose and infused at the end of CPB. Cardioplegia was applied at the surgeon's discretion. Lost blood was recovered using Cell Saver® Elite® (Haemonetics™, France) and re-transfused when possible. Vasotropic or inotropic agents, fluids and transfusion products were administered at the discretion of the anesthesiologist based on clinical, echocardiographic and biological findings. After surgery, all patients were transferred to the cardiovascular intensive care unit (ICU).

2.4. Prospective Sample and Data Collection

Urine samples were collected from a urinary catheter at 3 different times: (1) after the induction of anesthesia and before the start of CPB, (2) at the end of the CPB procedure, and (3) on the day after surgery in the ICU. Urine samples were collected in Corning 50-ml conical tubes and centrifuged at 2000g for 20 min within 4 h of collection. Cell pellets were conserved in 300 μL of RLT® buffer (Qiagen™, France) and stored until mRNA extraction. Supernatants and cell pellets were stored at −80 °C until analysis. Hemodynamic data were extracted from the Philips system using IXTREND® software version 2.1.0 FW14 (Ixellence GmbH, Germany). MAP values were recorded every 1.25 s during the CPB procedure. Clinical data were prospectively extracted from the hospital's electronic medical records. All clinical data and samples were de-identified.

2.5. ^{1}H NMR Spectroscopy

Urine samples were prepared to obtain a final volume of 600 μl (400 μl of urine; 160 μl of 200 mM phosphate buffer, pH 7.4; 1 mM trimethyl silyl propionate, sodium salt (TSP) as the NMR chemical shift reference, 6 mM NaN₃; and 40 μl of D₂O). Urine ^{1}H NMR spectra were measured at 300 K on a Bruker Avance II® 500 MHz spectrometer (Bruker Biospin GmbH, Germany) equipped with a SampleXpress® automation sample changer and a standard 5 mm broadband inverse (BBI) probe with a Z-gradient. The spectra were acquired using a 1D nuclear Overhauser effect spectroscopy (NOESY) pulse sequence with presaturation for water suppression. The parameters used for the pulse sequence were: a relaxation delay of 1 s, a mixing time of 100 ms, an acquisition time of 1.36 s and a 90° pulse length of 8 μs. Data points (32K) were collected during 64 scans with a spectral width of 20 ppm.

Preprocessing of the urine ^{1}H NMR spectra was performed with MestReNova® 8.0 software. A line-broadening factor of 0.3 Hz was applied prior to Fourier transform. The spectra were then phased, baseline corrected, and referenced to TSP. Each ^{1}H NMR spectrum (0.24 to 10.00 ppm) was reduced by an equidistant binning method with a bin width of 0.04 ppm to limit misalignment problems. The spectral regions corresponding to urea (5.52 to 6.04 ppm) and water (4.28 to 5.24 ppm) were deleted to remove variability because of the suppression of water. Integral normalization (typically a constant integral of 100) was performed on the remaining 210 bins. The resulting matrix was normalized with a commonly applied method for equidistant binned spectra, Pareto scaling, by dividing the mean-centered variables (bins) by the square root of their standard deviations.

2.6. Fragment Analysis of Urine sXBP1 and XBP1 mRNA Levels

RNA was extracted from the pellets using the RNeasy mini kit® (Qiagen™) and reverse-transcribed into cDNAs using TaqMan® Reverse

Transcription Reagents (Applied Biosystems™). Basically, the fragment analysis involved the following 3 steps:

(1) Amplification of the sXBP1 and XBP1 cDNAs by PCR using fluorogenic oligonucleotide primers. Several differently colored fluorescent dyes are detectable in one sample. We designed the following fluorogenic oligonucleotide primers (tagged with hexachloro-fluorescein, HEX, green) for the fluorometric detection of sXBP1 and XBP1 mRNA levels: Forward primer: (5′-HEX)GGAGTTAAGACAGCGCTTGG and Reverse Primer: GAGATGTTCTGGAGGGGTGA. We performed PCR using HotStar Taq® DNA polymerase on a thermal cycler with the following program: 95 °C for 10 min; 40 cycles of 94 °C for 30 s, 59 °C for 30 s, and 72 °C for 30 s; and a final step of 72 °C for 10 min.
(2) Labeled fragments (amplicons) were separated by size using capillary electrophoresis and the fluorescence intensity was

Table 1
Description of the cohort undergoing cardiac surgery.

Characteristics	All (n = 42)	AKI (n = 12)	No AKI (n = 30)	P value
Age (years)	62.1 ± 15.3	64.3 ± 4.4	61.3 ± 2.8	0.56
Men, n (%)	26 (62)	6 (50)	20 (66)	0.31
BMI (kg/cm²)	25.8 ± 4.9	27 ± 0.4	25.3 ± 0.9	0.31
Preexisting medical condition, n (%)				
• Hypertension	21 (50)	7 (58)	14 (46)	0.49
• Diabetes	2 (4.7)	1 (3)	1 (8)	0.5
• Obesity	7 (16)	2 (16)	5 (16)	1
• Atherosclerotic disease	6 (14.2)	2 (16)	4 (16)	0.78
• CKD	9 (21)	4 (33)	5 (16)	0.28
Preoperative characteristics				
• eGFR (ml/min/1.73 m²)	73.9 ± 22.9	63 ± 6.3	78.3 ± 4	0.49
• Ejection fraction (%)	60.6 ± 9.4	62 ± 2.7	61.1 ± 1.7	0.57
• Cleveland score	2.5 ± 1.4	2.7 ± 0.4	2.4 ± 0.2	0.52
• Euroscore 2[a]	2.7 ± 2.8	3.2 ± 0.8	2.5 ± 0.5	0.47
Preoperative medications, n (%)				
• RAS inhibitors	18 (43)	4 (33)	14 (46)	0.4
• Diuretics	12 (28)	7 (23)	5 (41)	0.27
• Beta blockers	22 (52)	8 (66)	14 (46)	0.26
Indications, n (%)				
• CABG	11 (26)	5 (41)	6 (20)	0.15
• Mitral valve	8 (19)	6 (20)	2 (16)	0.81
• Aortic valve	24 (57)	8 (66)	16 (66)	0.43
• Ascending aorta	6 (14)	1 (8)	5 (16)	0.46
• Others	6 (14)	1 (8)	5 (16)	0.46
Operative parameters				
• CBP length (min)	99.3 ± 22.9	109 ± 10.4	95 ± 6.5	0.25
• Aortic cross-clamp length (min)	75.1 ± 30.7	84 ± 8.8	71.6 ± 5.6	0.25
• Whole procedure length (min)	294.5 ± 45.2	311.6 ± 12.8	287.6 ± 8.1	0.12
• Fluid loading (ml)	1561.9 ± 708.8	1250 ± 198	1686.6 ± 125.7	0.07
• Blood loss (ml)	3014.9 ± 1382	3277.1 ± 419.4	2908.1 ± 267.7	0.46
• Cell saver (ml)	799.6 ± 620.8	692.2 ± 188.5	843.4 ± 120.3	0.5
• Per CBP urine output (ml/kg/h)	62.5 ± 87.5	64.7 ± 25.5	61.6 ± 16.1	0.9
• Per procedure urine output (ml/kg/h)	145 ± 106.5	162.1 ± 30.9	137.9 ± 19.9	0.51
Post-operative parameters				
• 24 h fluids administration (ml)[b]	2005 ± 737	2145 ± 214	1950 ± 135	0.5
• Catecholamine use (days)[c]	0.7 ± 1.1	1.2 ± 0.3	0.5 ± 1.1	0.05
• Dialysis, n (%)	3 (7)	3 (25)	0 (0)	0.004
• ICU stay (days)	3.5 ± 3.7	5.3 ± 1	2.8 ± 0.6	0.04
• Hospital stay (days)	15.3 ± 8.6	19.5 ± 9.5	13.7 ± 1.5	0.04
• Death, n (%)	2 (5)	2 (16)	0 (0)	0.02

Plus-minus values are means ± standard deviation.
BMI denotes body mass index; DSA, donor-specific antibodies; CKD, chronic kidney disease; eGFR, estimated glomerular filtration rate; RAS, renin-angiotensin system; CABG, coronary artery bypass grafting; CPB, cardiopulmonary bypass; ICU, intensive care unit.

[a] Euroscore 2, www.euroscore.org/calc.html.
[b] Includes albumin, Ringer's lactate, plasmion, or G5%.
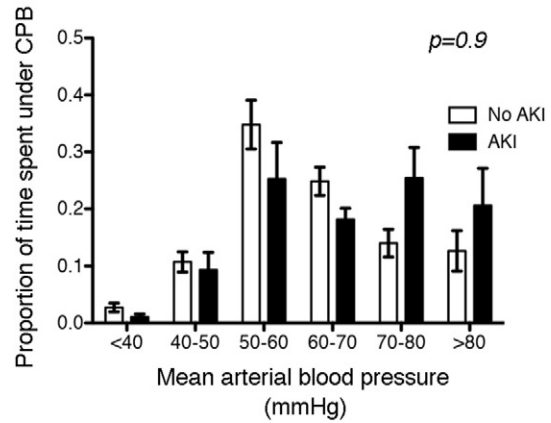[c] Includes norepinephrine, dobutamine or adrenaline.

Fig. 1. Time spent at a given mean arterial blood pressure and acute kidney injury occurrence. Histograms present the proportions of time spent at a given mean arterial blood pressure during cardiopulmonary bypass registered in real-time using XTrend® software, according to the occurrence of acute kidney injury, which were compared using a two-way ANOVA.

measured using the Applied Biosystems™ 3730xl DNA Analyzer. One of the dye colors (GENESCAN® ROX 400 HD size standard, Applied Biosystems™, red) is used to detect a labeled size standard present in each sample. Fragments and ROX 400 HD are mixed with HiDi™ Formamide (Applied Biosystems™) prior to capillary electrophoresis.

(3) The data were analyzed using GeneMapper® Software to determine the relative size of each dye-labeled fragment in the sample by comparing fragments with the standard curve for that specific sample.
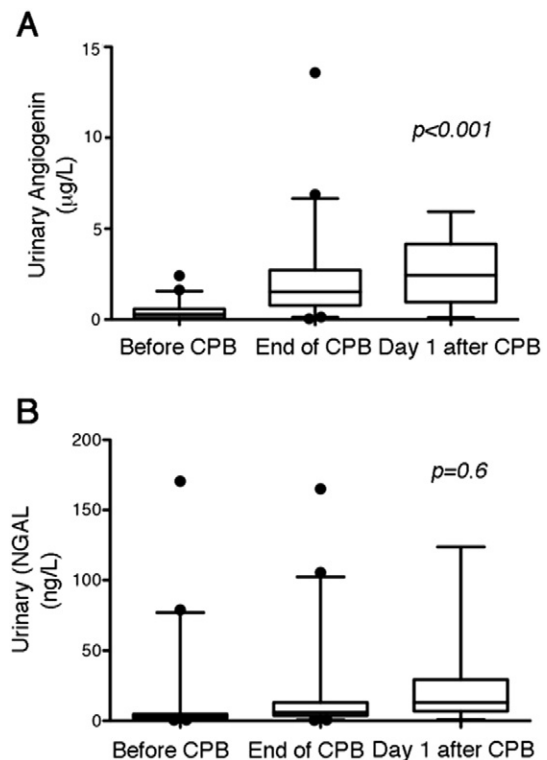

Fig. 2. Expression of markers of Endoplasmic Reticulum stress in urines during the procedure. A. Box and whisker plots present the distribution of angiogenin concentrations in the urine of 42 individuals undergoing cardiac surgery before, at the end and the day after CPB, which were compared using one-way ANOVA. B. Box and whisker plots present the distribution of NGAL concentrations in the urine of 42 individuals undergoing cardiac surgery before, at the end and on the day after CPB, which were compared using one-way ANOVA.
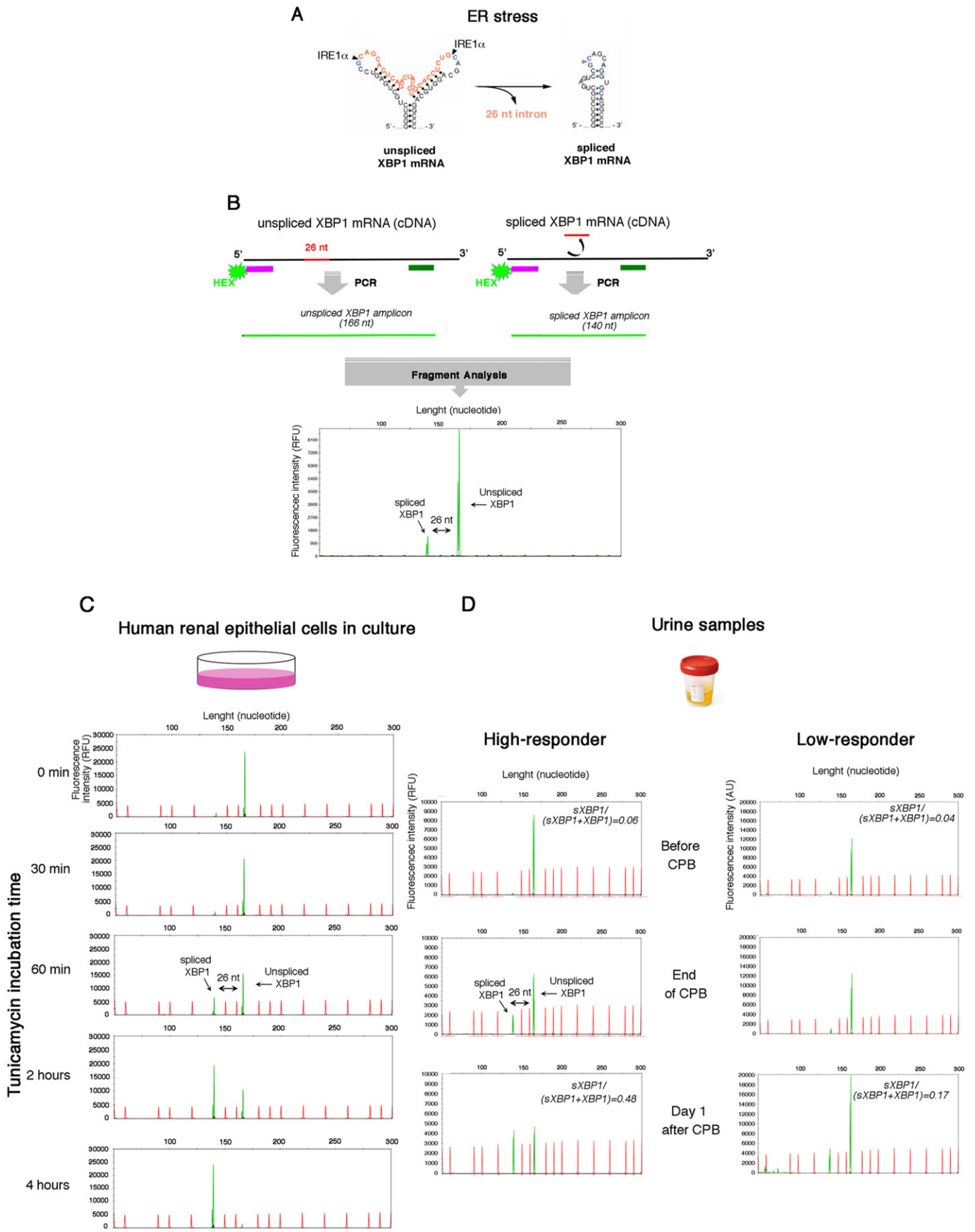
Fig. 3 *(Caption on next page)*

2.7. Urinary Angiogenin and NGAL Measurements

Urinary angiogenin and NGAL levels were quantified using the human Angiogenin and Lipocalin-2/NGAL Quantikine® ELISA Immunoassays (R&D Systems, USA), according to the manufacturer's protocol. Since the urinary angiogenin and NGAL concentrations were strongly correlated with their respective ratios with the corresponding urinary creatinine concentration (not shown), we did not adjust the values for the urinary creatinine concentration.

2.8. Statistical Analysis

Continuous variables are presented as the mean and standard deviation and categorical variables are presented as presented as proportions. Student's t-test was used to analyze the variance of continuous variables between different groups. Dichotomous variables were compared using the chi-square test. One-way and two-way ANOVAs were used to compare multiple mean values. Statistical analyses were performed using JMP 10® software (SAS, USA). All tests were two-sided, and P values < 0.05 were considered to indicate a significant difference.

Unsupervised analysis of metabolomic data has been performed using the PCA method with the SIMCA® 13.0 software (Umetrics™ AB, Sweden). Quality controls of the data were performed by deriving the principal component and its corresponding limits for the Hotelling's T^2 ellipse (strong outliers) and model residuals by using Distance in the Model in X space (DModX, moderate outliers) at the 99% confidence level. The models were evaluated with R^2X to estimate the goodness of the fit, and Q^2X estimate of the predictive ability of the model.

3. Results

3.1. Description of the Cohort and AKI Occurrence

We conducted a single-center, prospective study and enrolled 42 patients undergoing scheduled cardiac surgery with CPB. Baseline information, pre-operative parameters and post-operative outcomes are detailed in Table 1. The notable characteristic of this cohort is that AKI, as defined by the KDIGO Clinical Practice Guideline for Acute Kidney Injury criteria (http://kdigo.org/), occurred in 28% (n = 12) of patients. Two patients died at least 7 days after surgery. The mean CPB duration was 99 ± 36 min and the mean aortic cross-clamp duration was 75 ± 30 min, but neither of these parameters were associated with AKI occurrence. Real-time mean arterial pressure (MAP) recordings collected during the CPB procedure using IXTREND© monitoring software indicated that the mean arterial blood pressure had no impact on the occurrence of AKI in our cohort (Fig. 1). As expected, baseline renal function (before CPB) influenced the occurrence of AKI. The mean estimated glomerular filtration rate (eGFR) was 78 ± 24 ml/min/1.73 m² in individuals without AKI compared with 63 ± 13, 78 ± 24 ml/min/1.73 m² in individuals with AKI (p = 0.01 with Student's t-test). None of the other parameters that could impact renal function after CBP did influence AKI occurrence in our cohort (Table 1).

3.2. Real Time Monitoring of ER Stress by the Detection of sXBP1 in Urine

The engagement of an adaptive program defined by early activation of the ER stress response could affect the amplitude of the injury and the renal outcomes. We repeatedly measured the urine angiogenin concentrations (an indirect marker of the activity of the IRE1α/sXBP1 axis) (Tavernier et al., 2017) and neutrophil gelatinase-activated lipocalin (NGAL), which is regulated by the PERK/ATF4 pathway (El Karoui et al., 2016), to obtain additional information about the activation of the UPR during the CPB procedure. Notably, there is no known non-invasive biomarker that is produced and secreted in urine under the control of ATF6. Urine angiogenin concentrations increased significantly over time (Fig. 2A), but NGAL concentrations did not (Fig. 2B), indicating that the IRE1α/sXBP1 axis, rather than the PERK/ATF4 axis of the UPR appears to be activated in our cohort under these specific hemodynamic conditions.

We developed a method for measuring sXBP1 mRNA levels in urine (cell pellets) to provide definitive evidence that UPR activation following a hemodynamic impairment can be directly and non-invasively monitored. Because the XBP1 mRNA is 26 nucleotides longer than sXBP1 (Fig. 3A), we adopted a genetic marker analysis experiment (fragment analysis) to detect changes in the length of the XBP1 mRNA before and after splicing using PCR with fluorescent dye-labeled primers specific for the XBP1 coding sequence (Fig. 3B). Then, the PCR amplicons are separated according to their sizes and analyzed on a capillary electrophoresis-based DNA sequencing instrument. The fragment (amplicon) corresponding to the unspliced XBP1 mRNA is predicted to be 166 nucleotides, whereas the fragment (amplicon) corresponding to spliced XBP mRNA is predicted to contain 140 nucleotides (Fig. 3B).

We validated the biological relevance of this method in vitro using cultured human epithelial cells incubated with tunicamycin, a molecule that inhibits N-linked glycosylation and promotes ER stress (Marciniak et al., 2004). In untreated resting cells, sXBP1 was not detected. However, it progressively appeared after 60 min of tunicamycin exposure, and the intensity of the fluorescent peak increased for up to 4 h, and the intensity of the unspliced XBP1 peak progressively decreased (Fig. 3C).

We obtained similar profiles in the urine pellets of individuals undergoing CPB with an incremental increase in the peak intensities of sXBP1 (before, immediately after and one day after CPB), along with a parallel decrease in the intensities of the XBP1 peak (Fig. 3D, left panel). We also identified individuals in whom urinary sXBP1 levels with a much more moderate increase during the procedure, who were called "Low-responder" in Fig. 4D (right panel).

We calculated the ratio of sXBP1/(sXBP1 + XBP1) for each sample and used it as a proxy of the intensity of the UPR to determine the clinical relevance of the differences in the levels of sXBP1 among individuals undergoing CPB; one advantage is that this parameter does not depend on the urine concentration and does not require the use of a housekeeping gene for interpretation. These ratios significantly increased following CBP (Fig. 4A), confirming that hemodynamic impairments initiate ER stress and sXBP1 expression.

In addition, individuals who experienced AKI episodes exhibited a lower increase in sXBP1 ratios from the beginning to the end of CPB than individuals who did not experience AKI (Fig. 4B), suggesting that robust and early activation of the IRE1α/sXBP1 axis likely protects against AKI. In line with this, no AKI episode was observed in patients with a CPB sXBP1/(sXBP1 + XBP1) ratio increased at least 2 fold before/after CPB (c statistic 0.82, 95%IC, 0.61 to 1) (Table 2). However, values below these cutoffs have a low discriminative value and cannot predict the occurrence of AKI in patients at risk. Together, these results indicate that the detection of a strong adaptive response by the mean of

Fig. 3. Real time monitoring of Endoplasmic Reticulum stress by the detection of sXBP1 in urine. A. Schematic representing the excision of a 26 nucleotide intron from the XBP1 mRNA by IRE1α upon ER stress, resulting in the spliced form of XBP1, sXBP1. B. Graphical summarization of the principles of the fragment analysis used to detect XBP1 mRNA. C. The pattern of peaks resulting from the fragment analysis using capillary electrophoresis with GeneMapper©. Green peaks denote XBP1 (166 nucleotides) and sXBP1 (140 nucleotides) amplicons. Red peaks denote the size standards. The height of each peak corresponds to its relative fluorescence intensity. The x-axis denotes the fragment size. Total mRNAs were extracted from cultured renal epithelial cells that had been incubated with 2.5 μg/ml tunicamycin for various periods of time to induce ER stress. D. The pattern of peaks resulting from the fragment analysis performed on mRNA extracted from urinary cell pellets in individuals undergoing CPB. "High-responder" patients show the incremental conversion of unspliced XBP1 to spliced XBP1 over time (left panel), but "Low-responder" patients fail to show significant increase in sXBP1/(sXBP1/XBP1) levels (right panel).

urinary sXBP1 monitoring is predictive of a protection against AKI, but that a response of low intensity has a limited value for identifying patients who will develop AKI.

3.3. CPB Promotes Metabolic Reprogramming and Impacts Urinary Metabolomic Profiles

We postulate that the metabolic reprogramming processes within adaptive responses that are engaged early after the initiation of hemodynamic stress display distinct activation profiles, possibly resulting in different activities of the ER stress response. We compared the urinary metabolomic signatures (interpreted as a readout of ongoing cellular metabolic reprogramming in the kidney) of patients undergoing CPB using proton-based nuclear magnetic resonance (^{1}H NMR) spectroscopy. This technique allows the rapid, reproducible and comprehensive characterization of small molecules in urine and generates metabolic fingerprints, but it is less effective than mass spectrometry-based methods at identifying specific molecules and potential biomarkers (Beckonert et al., 2007; Lindon and Nicholson, 2008; Barding Jr et al., 2012; Zhang et al., 2012). Principal component analysis (PCA) of the 126 (42x3) urinary metabolomes of the 42 patients before CPB (at the time of anesthesia induction, shown in green in Fig. 5A), at the end of the CPB (shown in blue in Fig. 5A), and on the day after the surgical procedure (shown in red in Fig. 5A) illustrates the displacement of the individuals along the 2 principal component axes due to qualitative metabolomic changes that occur within urine during the procedure. Thus, in a few hours (mean CPB, 99 ± 36 min), CPB promotes renal metabolic reprogramming and profoundly alters the urinary metabolome. Notably, these profiles are not influenced by variations in urine concentration because each metabolome is completely normalized and compared as a whole.

Moreover, a group of patients displayed extreme qualitative metabolomic changes from the beginning to the end of CPB (Fig. 5B, circled in pale red, and Fig. 5C, left panel). Since metabolic reprogramming is a hallmark of the activation of adaptive responses to ischemia and is contingent on ER stress, we tested whether variations in the ER stress response be associated with these metabolic changes. The group of patients (Metabo group 1, n = 14), who displayed the highest metabolomics variations compared with their baseline values had significantly lower sXBP1/(sXBP1 + XBP1) ratio levels at the end of CPB compared the rest of the cohort (Fig. 5D), indicating that individuals who activate a robust ER stress response do not exhibit an early metabolic reprogramming.

Together, these results indicate that individuals differentially activate adaptive responses upon renal ischemic stress that are defined by early metabolic reprogramming and activation of the ER stress response. However, the relationship between ER stress and metabolic reprogramming, and the impact of ER stress in shaping cellular metabolic profiles, remain to be determined.

4. Discussion

We performed a biomarker analysis based on the assumption that biomarkers reflect specific biological processes occurring at the cellular level rather than serving primarily as tools to predict outcomes. Our interpretation of the qualitative and quantitative expression patterns described throughout the study is that specific adaptive responses occur very early after the initiation of CPB, a procedure potentially leading to AKI (which occurred in one-third of the patients in our cohort), regardless of the intensity and duration of the stress (for instance, the depth and duration of the hypotension during CPB). Instead, other parameters, such as the transient lack of arterial pulse pressure or CPB-induced inflammation, could be the main contributors to stress responses (Kumar and Suneja, 2011).

Our ER stress monitoring studies converge toward the concept that adaptive cellular responses that are engaged very early after an ischemic
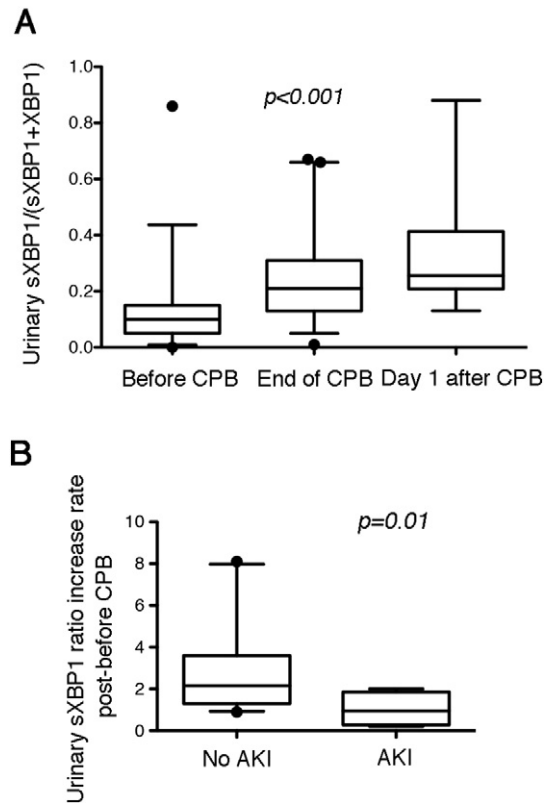
Fig. 4. Urinary sXBP1 and acute kidney injury. A. Box and whisker plots present the distribution of sXBP1/(sXBP1 + XBP1) in the urine of 42 individuals undergoing cardiac surgery before, at the end and on the day after CPB, which were compared using one-way ANOVA. B. Box and whisker plots present the distribution of the sXBP1/(sXBP1 + XBP1) variation rate according the occurrence of AKI in the urine of 42 individuals undergoing cardiac surgery after CPB compared to baseline, which were compared using Student's t-test.

insult are required to protect against tissue damage (notably, cell death and tissue remodeling), and individuals who, for as yet unknown reasons, are not able to mount a robust adaptive response are less protected against AKI and have a worse renal prognosis. This concept is consistent with the "preconditioning" hypothesis in which repeated small insults (including those that promote ER stress (Inagi et al., 2008, Liu et al., 2016, Usuki et al., 2013)) prior to a major injury may afford protection to the target tissue, in part because adaptive responses are already engaged (Hertzberg et al., 2017; Stokfisz et al., 2017). An understanding of the ability to activate these early responses is critical to correctly identify individuals at risk, which is likely due to complex interactions between intrinsic factors (e.g., genetic and epigenetic factors), acquired structural lesions (e.g., CKD), and environmental triggers (the nature, intensity and duration of the stressor). Consistent with this hypothesis, individuals with tubular atrophy (as observed during CKD) are less responsive to acute injury because of a lack of adaptive

Table 2
Performance of sXBP1 ratio and sXBP1 ratio increase rate to predict acute kidney injury.

Characteristics	Post-pre CPB sXBP1 ratio increase rate, %[a]
Sensitivity	100
Specificity	55
PPV	30
NPV	100

PPV, positive predictive value; NPV, negative predictive value.
[a] post CPB sXBP1/(sXBP1 + XBP1) divided by pre CPB sXBP1/(sXBP1 + XBP1), for a cutoff value of 2.
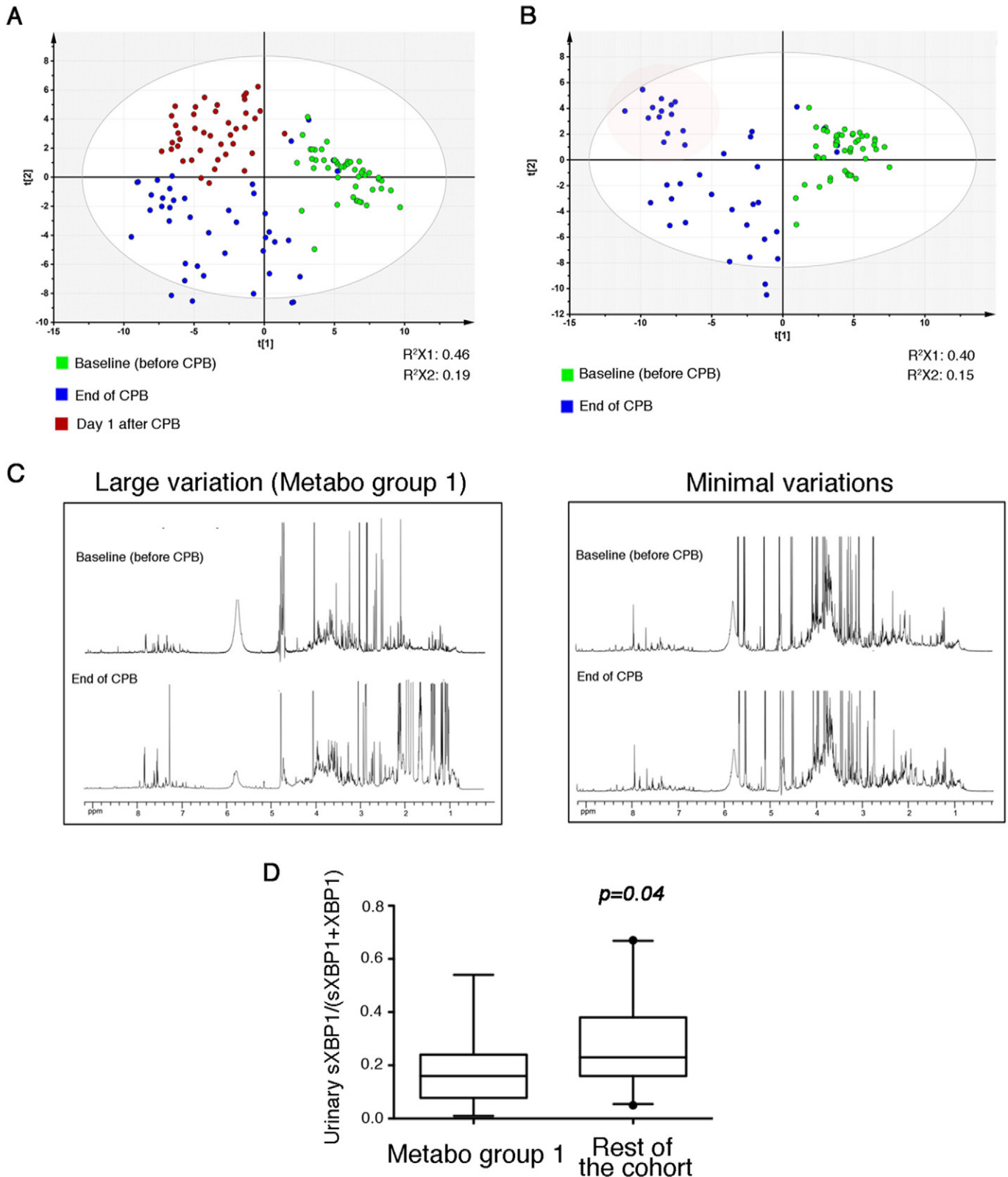
Fig. 5. Impact of cardiopulmonary bypass on metabolic reprogramming and urinary metabolomic profiles. A. Principal component analysis (PCA) of 126 urine samples collected from 42 individuals (42 after the induction of anesthesia and before the start of cardiopulmonary bypass (CPB), 42 at the end of the CPB procedure, and 42 on the day after surgery in the intensive care unit). Each point represents a sample (210 buckets from the ^{1}H-nuclear magnetic resonance spectrum, NMR). Green points represent urine samples at the time of anesthesia induction, blue points represent urine samples at the end of CPB, and red points indicate urine samples collected on the day after CPB. Model characteristics: R^2, 0.92; Q^2, 0.65. B. PCA of urine samples collected after the induction of anesthesia and at the end of CPB. Samples from 2 individual patients are highlighted in the PCA: patient A, with virtually no variation in the metabolome before and after CPB, and patient B, with a large variation in the metabolome before and after CPB. The red circle defines 13 samples with larger variations compared with the baseline. Model characteristics: $R^2 = 0.93$, $Q^2 = 0.64$. C. Representative ^{1}H NMR spectra of urine from patients A and B before and after CPB. D. Box and whisker plots present the distribution of sXBP1/(sXBP1 + XBP1) ratio following CPB in the 42 individuals undergoing cardiac surgery, according to Metabo groups, which were compared using Student's t-test.

fitness due to permanent epithelial homeostatic disturbances and phenotypic changes (Chawla et al., 2014). Finally, these findings underscore the absolute need to appreciate the biological significance of biomarker monitoring and the timing of responses. The expression levels of markers of cell death, such as kidney injury molecule 1 (KIM-1), or markers of tissue remodeling, such as matrix metalloproteinase 7 (MMP7, a marker of the activation of the WNT-β catenin pathway), are predictors of poor outcomes, including AKI (Alge and Arthur, 2015; Yang et al., 2017). The expression levels of markers of beneficial (but transient) adaptive responses, such as ER stress, are predictors of better outcomes. In line with this, the activation of other adaptive molecular pathways, such as the mammalian target of rapamycin complexes (MTORC) 1- and 2-mediated signaling pathways, are beneficial in patients with kidney injuries (Canaud et al., 2013; Godel et al., 2011; Inoki et al., 2011), although non-invasive markers of their activation still await development. The prognostic value of the markers of the ER stress response may also change with the duration of adaptive responses, which also reflect the length of the stress. Excessively prolonged ER stress responses promote cell death as a result of an imbalance in favor of proapoptotic pathways rather than antiapoptotic pathways as dynamic forces evolve over time toward the elimination of the stressed cell (Walter and Ron, 2011).

From a technological perspective, we report the first direct and non-invasive method for monitoring ER stress and the UPR. Since sXBP1 production exclusively depends on IRE1A, it is the best possible surrogate marker of ER stress. The protocol is simple, and inexpensive. More importantly, it has been exclusively performed within the Clinical Chemistry Department of the hospital, indicating that routine clinical applications are immediately feasible, provided that a molecular genetics platform is available. Considering the growing number of conditions in which ER stress is involved, including renal diseases (podocytopathies, interstitial fibrosis, nephrotoxicity, chronic proteinuria, autosomal dominant polycystic kidney disease, ischemic AKI, and kidney transplantation), our findings will undoubtedly pave the way for the implementation of translational applications.

In conclusion, this proof-of-concept study demonstrates the feasibility of the non-invasive detection of the ER stress response in urine in patients undergoing cardiac surgery under CPB and indicates that an early and robust adaptive response is critical for endogenous nephroprotection. The detection of urine sXBP1 levels is a straightforward method for monitoring renal ER stress. Larger studies will be performed to determine the clinical significance of monitoring ER stress with urinary sXBP1 levels as a proxy and will delineate the range of medical conditions that can be monitored with this detection tool.

Supplementary data to this article can be found online at https://doi.org/10.1016/j.ebiom.2017.12.023.

Funding Sources

Conflicts of Interest

The authors have no conflict of interest to disclose.

References

Alge, J.L., Arthur, J.M., 2015. Biomarkers of AKI: a review of mechanistic relevance and potential therapeutic implications. Clin. J. Am. Soc. Nephrol. 10 (1), 147–155.

Barding Jr., G.A., Salditos, R., Larive, C.K., 2012. Quantitative NMR for bioanalysis and metabolomics. Anal. Bioanal. Chem. 404 (4), 1165–1179.

Beckonert, O., Keun, H.C., Ebbels, T.M., Bundy, J., Holmes, E., Lindon, J.C., Nicholson, J.K., 2007. Metabolic profiling, metabolomic and metabonomic procedures for NMR spectroscopy of urine, plasma, serum and tissue extracts. Nat. Protoc. 2 (11), 2692–2703.

Bonventre, J., Zuk, A., 2004. Ischemic acute renal failure: an inflammatory disease? Kidney Int. 66 (2), 480–485.

Canaud, G., Bienaime, F., Viau, A., Treins, C., Baron, W., Nguyen, C., Burtin, M., Berissi, S., Giannakakis, K., Muda, A.O., Zschiedrich, S., Huber, T.B., Friedlander, G., Legendre, C., Pontoglio, M., Pende, M., Terzi, F., 2013. AKT2 is essential to maintain podocyte viability and function during chronic kidney disease. Nat. Med. 19 (10), 1288–1296.

Chawla, L.S., Eggers, P.W., Star, R.A., Kimmel, P.L., 2014. Acute kidney injury and chronic kidney disease as interconnected syndromes. N. Engl. J. Med. 371 (1), 58–66.

Chen, X., Iliopoulos, D., Zhang, Q., Tang, Q., Greenblatt, M.B., Hatziapostolou, M., Lim, E., Tam, W.L., Ni, M., Chen, Y., Mai, J., Shen, H., Hu, D.Z., Adoro, S., Hu, B., Song, M., Tan, C., Landis, M.D., Ferrari, M., Shin, S.J., Brown, M., Chang, J.C., Liu, X.S., Glimcher, L.H., 2014. XBP1 promotes triple-negative breast cancer by controlling the HIF1alpha pathway. Nature 508 (7494), 103–107.

Chovatiya, R., Medzhitov, R., 2014. Stress, inflammation, and defense of homeostasis. Mol. Cell 54 (2), 281–288.

Cubillos-Ruiz, J.R., Silberman, P.C., Rutkowski, M.R., Chopra, S., Perales-Puchalt, A., Song, M., Zhang, S., Bettigole, S.E., Gupta, D., Holcomb, K., Ellenson, L.H., Caputo, T., Lee, A.H., Conejo-Garcia, J.R., Glimcher, L.H., 2015. ER stress sensor XBP1 controls anti-tumor immunity by disrupting dendritic cell homeostasis. Cell 161 (7), 1527–1538.

Duffield, J.S., 2014. Cellular and molecular mechanisms in kidney fibrosis. J. Clin. Invest. 124 (6), 2299–2306.

El Karoui, K., Viau, A., Dellis, O., Bagattin, A., Nguyen, C., Baron, W., Burtin, M., Broueilh, M., Heidet, L., Mollet, G., Druilhe, A., Antignac, C., Knebelmann, B., Friedlander, G., Bienaime, F., Gallazzini, M., Terzi, F., 2016. Endoplasmic reticulum stress drives proteinuria-induced kidney lesions via Lipocalin 2. Nat. Commun. 7, 10330.

Ferenbach, D.A., Bonventre, J.V., 2015. Mechanisms of maladaptive repair after AKI leading to accelerated kidney ageing and CKD. Nat. Rev. Nephrol. 11 (5), 264–276.

Gao, X.H., Krokowski, D., Guan, B.J., Bederman, I., Majumder, M., Parisien, M., Diatchenko, L., Kabil, O., Willard, B., Banerjee, R., Wang, B., Bebek, G., Evans, C.R., Fox, P.L., Gerson, S.L., Hoppel, C.L., Liu, M., Arvan, P., Hatzoglou, M., 2015. Quantitative H2S-mediated protein sulfhydration reveals metabolic reprogramming during the integrated stress response. elife 4, e10067.

Godel, M., Hartleben, B., Herbach, N., Liu, S., Zschiedrich, S., Lu, S., Debreczeni-Mor, A., Lindenmeyer, M.T., Rastaldi, M.P., Hartleben, G., Wiech, T., Fornoni, A., Nelson, R.G., Kretzler, M., Wanke, R., Pavenstadt, H., Kerjaschki, D., Cohen, C.D., Hall, M.N., Ruegg, M.A., Inoki, K., Walz, G., Huber, T.B., 2011. Role of mTOR in podocyte function and diabetic nephropathy in humans and mice. J. Clin. Invest. 121 (6), 2197–2209.

Hertzberg, D., Ryden, L., Pickering, J.W., Sartipy, U., Holzmann, M.J., 2017. Acute kidney injury-an overview of diagnostic methods and clinical management. Clin. Kidney J. 10 (3), 323–331.

Hetz, C., Glimcher, L.H., 2009. Fine-tuning of the unfolded protein response: assembling the IRE1alpha interactome. Mol. Cell 35 (5), 551–561.

Inagi, R., Kumagai, T., Nishi, H., Kawakami, T., Miyata, T., Fujita, T., Nangaku, M., 2008. Preconditioning with endoplasmic reticulum stress ameliorates mesangioproliferative glomerulonephritis. J. Am. Soc. Nephrol. 19 (5), 915–922.

Inagi, R., Ishimoto, Y., Nangaku, M., 2014. Proteostasis in endoplasmic reticulum—new mechanisms in kidney disease. Nat. Rev. Nephrol. 10 (7), 369–378.

Inoki, K., Mori, H., Wang, J., Suzuki, T., Hong, S., Yoshida, S., Blattner, S.M., Ikenoue, T., Ruegg, M.A., Hall, M.N., Kwiatkowski, D.J., Rastaldi, M.P., Huber, T.B., Kretzler, M., Holzman, L.B., Wiggins, R.C., Guan, K.L., 2011. mTORC1 activation in podocytes is a critical step in the development of diabetic nephropathy in mice. J. Clin. Invest. 121 (6), 2181–2196.

Kotas, M.E., Medzhitov, R., 2015. Homeostasis, inflammation, and disease susceptibility. Cell 160 (5), 816–827.

Kumar, A.B., Suneja, M., 2011. Cardiopulmonary bypass-associated acute kidney injury. Anesthesiology 114 (4), 964–970.

Lindon, J.C., Nicholson, J.K., 2008. Spectroscopic and statistical techniques for information recovery in metabonomics and metabolomics. Annu Rev Anal Chem (Palo Alto, Calif) 1, 45–69.

Liu, D., Liu, X., Zhou, T., Yao, W., Zhao, J., Zheng, Z., Jiang, W., Wang, F., Aikhionbare, F.O., Hill, D.L., Emmett, N., Guo, Z., Wang, D., Yao, X., Chen, Y., 2016. IRE1-RACK1 axis orchestrates ER stress preconditioning-elicited cytoprotection from ischemia/reperfusion injury in liver. J. Mol. Cell Biol. 8 (2), 144–156.

Mami, I., Bouvier, N., El Karoui, K., Gallazzini, M., Rabant, M., Laurent-Puig, P., Li, S., Tharaux, P.L., Beaune, P., Thervet, E., Chevet, E., Hu, G.F., Pallet, N., 2016a. Angiogenin mediates cell-autonomous translational control under endoplasmic reticulum stress and attenuates kidney injury. J. Am. Soc. Nephrol. 27 (3), 863–876.

Mami, I., Tavernier, Q., Bouvier, N., Aboukamis, R., Desbuissons, G., Rabant, M., Poindessous, V., Laurent-Puig, P., Beaune, P., Tharaux, P.L., Thervet, E., Chevet, E., Anglicheau, D., Pallet, N., 2016b. A novel extrinsic pathway for the unfolded protein response in the kidney. J. Am. Soc. Nephrol. 27 (9), 2670–2683.

Marciniak, S.J., Yun, C.Y., Oyadomari, S., Novoa, I., Zhang, Y., Jungreis, R., Nagata, K., Harding, H.P., Ron, D., 2004. CHOP induces death by promoting protein synthesis and oxidation in the stressed endoplasmic reticulum. Genes Dev. 18 (24), 3066–3077.

Martinon, F., Chen, X., Lee, A.H., Glimcher, L.H., 2010. TLR activation of the transcription factor XBP1 regulates innate immune responses in macrophages. Nat. Immunol. 11 (5), 411–418.

Stokfisz, K., Ledakowicz-Polak, A., Zagorski, M., Zielinska, M., 2017. Ischaemic preconditioning - current knowledge and potential future applications after 30 years of experience. Adv. Med. Sci. 62 (2), 307–316.

Tavernier, Q., Mami, I., Rabant, M., Karras, A., Laurent-Puig, P., Chevet, E., Thervet, E., Anglicheau, D., Pallet, N., 2017. Urinary angiogenin reflects the magnitude of kidney injury at the infrahistologic level. J. Am. Soc. Nephrol. 28 (2), 678–690.

Usuki, F., Fujimura, M., Yamashita, A., 2013. Endoplasmic reticulum stress preconditioning attenuates methylmercury-induced cellular damage by inducing favorable stress responses. Sci. Rep. 3 (2346).

Walter, P., Ron, D., 2011. The unfolded protein response: from stress pathway to homeostatic regulation. Science 334 (6059), 1081–1086.

Wang, M., Kaufman, R.J., 2016. Protein misfolding in the endoplasmic reticulum as a conduit to human disease. Nature 529 (7586), 326–335.

Wellen, K.E., Thompson, C.B., 2010. Cellular metabolic stress: considering how cells respond to nutrient excess. Mol. Cell 40 (2), 323–332.

Wu, R., Zhang, Q.H., Lu, Y.J., Ren, K., Yi, G.H., 2015. Involvement of the IRE1alpha-XBP1 pathway and XBP1s-dependent transcriptional reprogramming in metabolic diseases. DNA Cell Biol. 34 (1), 6–18.

Yang, X., Chen, C., Teng, S., Fu, X., Zha, Y., Liu, H., Wang, L., Tian, J., Zhang, X., Liu, Y., Nie, J., Hou, F.F., 2017. Urinary matrix metalloproteinase-7 predicts severe AKI and poor outcomes after cardiac surgery. J. Am. Soc. Nephrol. 28 (11), 3373–3382.

Zhang, A., Sun, H., Wang, X., 2012. Serum metabolomics as a novel diagnostic approach for disease: a systematic review. Anal. Bioanal. Chem. 404 (4), 1239–1245.

Zuk, A., Bonventre, J.V., 2016. Acute kidney injury. Annu. Rev. Med. 67, 293–307.